Proceedings of the 2016 IEEE
International Conference on Robotics and Biomimetics
Qingdao, China, December 3-7, 2016

Static Modeling and Analysis of Continuum Surgical Robots

Han YUAN, Zheng LI, Hongmin WANG and Chengzhi SONG

Abstract— **Continuum Robots have been investigated increasingly in recent years due to their potential applications in minimally invasive surgery (MIS). The constant curvature assumption is widely adopted in modeling the motion of continuum robots. However, due to their limited backbone rigidity, the backbone bending or end-effector position is significantly affected by both the internal driven force and external load. This paper focuses on the static analysis of the continuum robots. Statics model of the robot is established based on the Newton-Euler method. Gravity of the elastic tubes and the disks are both considered in the modeling. Based on the static model, the shape of the robot can be calculated with given external loads and internal driven force (i.e. cable tension). The model is validated using finite element method (FEM). The error is less than 0.02 percent. Simulation results reveal that, the shape of the robot is significantly affected by the external load. A S-type bending can be observed with certain loading conditions. Therefore, the commonly adopted constant curvature is invalid in loaded circumstances.**

I. INTRODUCTION

Minimally Invasive Surgery (MIS) becomes popular in the last few decades, since patients benefit a lot from MIS, such as less pain, lower cost, faster recovery [1], [2]. Recently, robots have been integrated in operating rooms world widely [2], [3]. With the help of robots, procedures of MIS have been greatly improved in various aspects: better precision, less operating time, remote operation, etc. During various robotic-assisted surgeries [4], the Da Vinci surgical system by Intuitive Surgical is one of the most widely used. From robotic view, Da Vince is a rigid-link manipulator. In order to achieve enough degrees of freedom, it has to be built with a lot of links and joints, which makes the Da Vinci system bulky, complex and expensive.

Besides rigid-link robots, continuum robots also have great potentials in robotic-assisted MIS. According to [5], a continuum robot is an actuatable structure whose constitutive material forms curves with continuous tangent vectors. Due to the flexible structure, continuum robots have big advantages on dexterity. Generally, three kinds of continuum robots can be considered according to their structures. Most of continuum robots are single backbone robots, which have one elastic part in the center to support the whole structure, such as the robots in [6], [7], [8], [9], [10], [11]. Similar design is also used in other robot designs, such as the robots in [12], [13], [14]. Another kind of continuum robots are multi-backbone robots. They have several parallel elastic elements running through the whole structure, such as the robots in [15], [16], [17]. Another continuum robots are the concentric tube robots, which have a set of concentric tubes with different pre-curvatures. Different bending can be achieved through rotating the tubes, such as the robots presented in [18], [19], [20]. This paper mainly presents the single backbone continuum robots. A center elastic tube is used as the central core. Inside the tube, various materials can pass through, such as the electric wires, controlling cables, etc. This structure makes the robot extensible to different tasks.

Static model is essential for the analysis of continuum robot. In view of robotics, continuum robot can be regarded as an under-actuated serial robot with hyper-redundant degrees of freedom. Thus, statics of this kind robot is coupled with robot kinematics, which makes modeling and analysis more complicated. Lots of previous researches focus on the kinematic analysis of continuum robots [21], [22], [23], [24], where the constant curvature assumption is widely adopted. With this assumption, the bending profile of the continuous robots is regarded as an arc. However, due to the large compliance of the continuum robots, the bending shape could be significantly affected by the external loading. In this situation, kinematic modeling with constant curvature assumption cannot predict the robot profile accurately. Therefore, static modeling considering external load is important. Static analysis of a multiple-backbone continuum robots is presented in [25], in which system static equilibrium is derived using elliptic integrals. Based on the Cosserat-rod theory, static models of continuum robots are proposed in [26], [27]. Static analysis of a single backbone continuum manipulator is made in [9], where static model is proposed based on the principle of virtual work and simulation results are presented and compared with finite element analysis.

This paper states on the static modeling and analysis of the single backbone continuum robots by Newton-Euler method. Effects of gravity and external loading are both taken into consideration. With this static model, the profile of the robot can be calculated with given controlling cable forces and external loads. In addition, finite element method is employed as a compassion, in order to validate the proposed model. Relationship among position of the robot end, driven cable forces and external loads is analyzed.

*This research is supported by the project SHIAE-8115049 of the Shun Hing Institute of Advanced Technology,the Chinese University of Hong Kong; the Hong Kong Innovative Technology Fund (ITF), with project No. ITS/019/15 and Hong Kong General Research Fund (GRF), with project No.14212316.

Han YUAN, Hongmin WANG and Chengzhi SONG are with the Institute of Digestive Disease and Chow Yuk Ho Technology Center for Innovative Medicine, the Chinese University of Hong Kong. Phone: +852-39434237. Email: han.yuan.robot@icloud.com

Zheng LI is with the Institute of Digestive Disease, Chow Yuk Ho Technology Center for Innovative Medicine and Biomedical Engineering Programme, the Chinese University of Hong Kong. Phone: +852-39434240. Email: lizheng@cuhk.edu.hk

Significant effect of the external loading on the static profile of the continuum robots is found. Under external loads, the constant curvature assumption is no longer valid. For example, a S-type bending is found under certain loading conditions, through our simulations based on the proposed model. The proposed model is significant for the analysis of continuum robots, such as improving the static positioning accuracy with different loading conditions.

This paper is organized as following. The typical structure of the single backbone continuum robots is firstly presented in Section II. Then static modeling is detailed in Section III, considering the coupling of statics and kinematics. Numerical analysis is made in Section IV through the proposed static model and the finite element method. Based on these results, discussions are presented in Section IV. Finally, conclusion is made in Section V.

II. STRUCTURE DESIGN

Most continuum robots used for medical applications are single backbone robots which have one central elastic part to support the whole structure. A typical structure of this kind of continuum robots is shown in Fig. 1. As we can see, a serial of disks are mounted on an elastic tube. Four driven cables pass through the holes in the disks, and cables move along the disk holes with very little friction. By changing the lengths and/or forces of the driven cables, the structure can achieve a desired bending. It should be noted that using elastic tube as the core structure gives the robot good extensible abilities. For example, various end-effectors, such as cameras, scissors and clamp, can be added at the end of the continuum robot. Controlling wires and/or electric wires of the end-effectors can pass through the elastic tube. In addition, disks and cables in this paper are made by low friction materials, such as Teflon and Nylon. Thus a frictionless assumption is made in the modeling part.

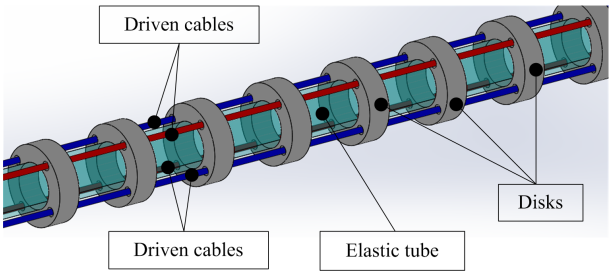

Fig. 1. Structure of the continuum robots.

Figure 2 illustrates a potential application of the continuum robots in minimally invasive surgery, where a handheld endoscope using a continuum bending section is designed. As shown in Fig. 2, the continuum section is attached to a rigid shaft and a handle. The movement of the continuum section can be controlled by a thumb steering on the handle. In this design, a wireless camera is mounted at the end of the continuum section. Different views by the camera can be achieved through the controllable bending of the continuum section. Furthermore, this handheld device can be extended for other tasks by using different medical instruments as end-effectors, such as scissors, forceps and hooks.

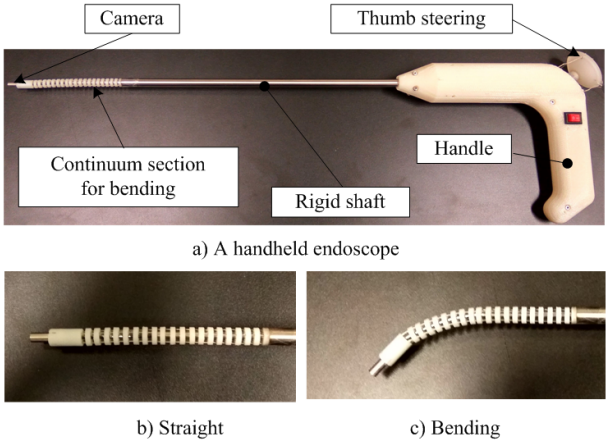

Fig. 2. Application of the continuum robot: handheld endoscope.

III. STATIC MODELING

The static model of a continuum robot is presented in this section. Coupling between the statics and kinematics is analyzed, which can be further expressed by a set of nonlinear equations. Optimization method is employed to get the solution. For convenience sake, analysis in this section is made in a plane. However, the proposed model is also extendable to three dimensions.

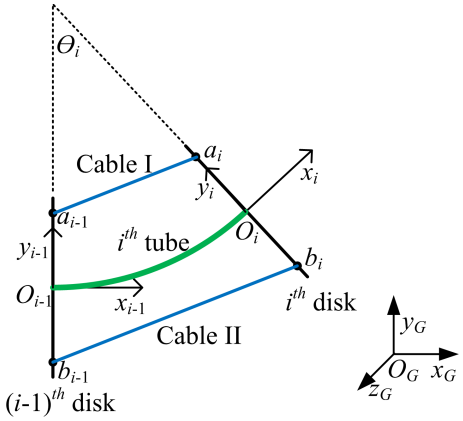

Fig. 3. The i^{th} segment of the continuum robot

Figure 3 shows the diagram of i^{th} segment of the continuum robot between two adjacent disks, the $(i-1)^{th}$ and i^{th} disks. Local frames Ro_{i-1} and Ro_i are fixed on the $(i-1)^{th}$ and i^{th} disks, respectively. Cable I and II provide the driven forces. The following assumptions are made.

- Since the stiffness of the elastic tube along the axis direction is much larger than the bending stiffness, elongation along the tube axis is ignored;
- The deformation of the elastic tube is pure bending;
- The elastic tube can be simulated by an Euler-Bernoulli beam;

- Profile of the elastic tube between two adjacent disks is approximated to an arc;
- Profile of the driven cable between two adjacent disks is straight lines.

Based on these assumptions, static analysis of the robot is made.

A. Force and moment analysis

(1) Force and moment by the driven cables:

The driven force along the i^{th} segment of cable I expressed in the local frame fixed with the $(i-1)^{th}$ disk Ro_{i-1} can be written as:

$$\mathbf{F}_{\mathrm{CI}i}^{R_{i-1}} = F_{\mathrm{CI}i} \cdot \frac{\overrightarrow{a_i a_{i-1}}^{R_{i-1}}}{|\overrightarrow{a_i a_{i-1}}^{R_{i-1}}|} + F_{\mathrm{CI}(i+1)} \cdot \frac{\overrightarrow{a_i a_{i+1}}^{R_{i-1}}}{|\overrightarrow{a_i a_{i+1}}^{R_{i-1}}|}, \quad (1)$$

where $i = 1, \cdots n-1$; $F_{\mathrm{CI}i}$ and $F_{\mathrm{CI}(i+1)}$ are the values of the driven forces along the i^{th} and $(i+1)^{th}$ segments of cable I. A special case is $i = n$, where the last disk of the robot is considered. Then the driven force will be:

$$\mathbf{F}_{\mathrm{CI}n}^{R_{n-1}} = F_{\mathrm{CI}n} \cdot \frac{\overrightarrow{a_n a_{n-1}}^{R_{n-1}}}{|\overrightarrow{a_n a_{n-1}}^{R_{n-1}}|}. \quad (2)$$

Similarly, the driven force along cable II expressed in the frame Ro_{i-1} can be written as: for $i = 1, \cdots n-1$,

$$\mathbf{F}_{\mathrm{CII}i}^{R_{i-1}} = F_{\mathrm{CII}i} \cdot \frac{\overrightarrow{b_i b_{i-1}}^{R_{i-1}}}{|\overrightarrow{b_i b_{i-1}}^{R_{i-1}}|} + F_{\mathrm{CII}(i+1)} \cdot \frac{\overrightarrow{b_i b_{i+1}}^{R_{i-1}}}{|\overrightarrow{b_i b_{i+1}}^{R_{i-1}}|}, \quad (3)$$

for $i = n$,

$$\mathbf{F}_{\mathrm{CII}n}^{R_{n-1}} = F_{\mathrm{CII}n} \cdot \frac{\overrightarrow{b_n b_{n-1}}^{R_{n-1}}}{|\overrightarrow{b_n b_{n-1}}^{R_{n-1}}|}. \quad (4)$$

The moment of the driven forces $\mathbf{F}_{\mathrm{CI}i}^{R_{i-1}}$ and $\mathbf{F}_{\mathrm{CII}i}^{R_{i-1}}$ relative to point o_{i-1} can be calculated as:

$$\mathbf{M}_{\mathrm{CI}i} = \overrightarrow{o_{i-1} a_i}^{R_{i-1}} \times \mathbf{F}_{\mathrm{CI}i}^{R_{i-1}} \quad (5)$$

$$\mathbf{M}_{\mathrm{CII}i} = \overrightarrow{o_{i-1} b_i}^{R_{i-1}} \times \mathbf{F}_{\mathrm{CII}i}^{R_{i-1}} \quad (6)$$

(2) Force and moment due to the gravity of the disks and tubes:

If the y axis of the global frame R_G is defined vertically upwards, the gravity of the i^{th} disk in R_G can be simply expressed as $\mathbf{G}_{\mathrm{d}i}^{R_G} = [0, -m_{\mathrm{d}i} \cdot g, 0]^{\mathrm{T}}$, where $m_{\mathrm{d}i}$ is the mass of the i^{th} disk. In order to obtain the expression of gravity in frame R_{i-1}, a transformation matrix ${}^{R_{i-1}}\mathrm{T}_{R_G}$ is defined, so that

$$\mathbf{G}_{\mathrm{d}i}^{R_{i-1}} = {}^{R_{i-1}}\mathrm{T}_{R_G} \cdot \mathbf{G}_{\mathrm{d}i}^{R_G} \ (i = 1, \cdots n), \quad (7)$$

in which

$${}^{R_{i-1}}\mathrm{T}_{R_G} = {}^{R_G}\mathrm{T}_{R_{i-1}}^{-1} = ({}^{R_G}\mathrm{T}_{R_0} \cdot {}^{R_0}\mathrm{T}_{R_{i-1}})^{-1}, \quad (8)$$

where ${}^{R_G}\mathrm{T}_{R_0}$ is the transformation matrix from frame R_0 to R_G, and the ${}^{R_0}\mathrm{T}_{R_{i-1}}$ is the transformation matrix from frame R_{i-1} to R_0. To calculate ${}^{R_0}\mathrm{T}_{R_{i-1}}$, the transformation matrix from frame R_q to R_p is defined as:

$${}^{R_p}\mathrm{T}_{R_q} = \prod_{i=p+1}^{q} {}^{R_{i-1}}\mathrm{T}_{R_i}, \quad (9)$$

$${}^{R_{i-1}}\mathrm{T}_{R_i} = \begin{bmatrix} \cos\theta_i & -\sin\theta_i & x_{o_i}^{R_{i-1}} \\ \sin\theta_i & \cos\theta_i & y_{o_i}^{R_{i-1}} \\ 0 & 0 & 1 \end{bmatrix}, \quad (10)$$

where $0 \le p < n,\ 0 < q \le n,\ p < q,\ 0 < i \le n$; $x_{o_i}^{R_{i-1}}$ and $y_{o_i}^{R_{i-1}}$ are respectively the x and y coordinates of point o_i in frame R_{i-1}. According to the geometric relationship shown in Fig. 3, $x_{o_i}^{R_{i-1}}$ and $y_{o_i}^{R_{i-1}}$ can be calculated by:

$$x_{o_i}^{R_{i-1}} = \frac{L_{0i}}{\theta_i} \cdot \sin\theta_i, \quad (11)$$

$$y_{o_i}^{R_{i-1}} = \frac{L_{0i}}{\theta_i} \cdot (1 - \cos\theta_i), \quad (12)$$

where L_{0i} is the length of the i^{th} tube, i.e. the arc length; θ_i is the rotation angle of the i^{th} tube, i.e. the angle of the arc in radians.

Similarly, the gravity of the i^{th} tube can be also expressed in the local frame R_{i-1}:

$$\mathbf{G}_{\mathrm{t}i}^{R_{i-1}} = {}^{R_{i-1}}\mathrm{T}_{R_G} \cdot \mathbf{G}_{\mathrm{t}i}^{R_G} \ (i = 1, \cdots n), \quad (13)$$

where $\mathbf{G}_{\mathrm{t}i}^{R_G}$ is the gravity of the i^{th} tube in R_G. $\mathbf{G}_{\mathrm{t}i}^{R_G}$ can be simply expressed as $\mathbf{G}_{\mathrm{t}i}^{R_G} = [0, -m_{\mathrm{t}i} \cdot g, 0]^{\mathrm{T}}$, and $m_{\mathrm{t}i}$ is the mass of the i^{th} tube.

Then, the moment of the disk gravity $\mathbf{G}_{\mathrm{d}i}^{R_{i-1}}$ relative to point o_{i-1} can be calculated as:

$$\mathbf{M}_{\mathrm{d}i} = \overrightarrow{o_{i-1} o_i}^{R_{i-1}} \times \mathbf{G}_{\mathrm{d}i}^{R_{i-1}}. \quad (14)$$

As for the moment of the tube gravity, the distance vector can be approximately equal to $\frac{\overrightarrow{o_{i-1} o_i}^{R_{i-1}}}{2}$. Thus the moment $\mathbf{M}_{\mathrm{t}i}$ can be calculated by:

$$\mathbf{M}_{\mathrm{t}i} = \frac{\overrightarrow{o_{i-1} o_i}^{R_{i-1}}}{2} \times \mathbf{G}_{\mathrm{t}i}^{R_{i-1}}. \quad (15)$$

B. Static equilibrium equations

In this sub-section, Newton-Euler formula is employed to obtain the static model. For the n^{th} segment of the robot, i.e. the last segment, external force and moment should be considered. According to the static equilibrium, the force and moment applied on point o_{n-1} can be calculated by:

$$\mathbf{F}_{o_{n-1}}^{R_{n-1}} = \mathbf{F}_{\mathrm{CI}n}^{R_{n-1}} + \mathbf{F}_{\mathrm{CII}n}^{R_{n-1}} + \mathbf{G}_{\mathrm{d}n}^{R_{n-1}} + \mathbf{G}_{\mathrm{t}n}^{R_{n-1}} + \mathbf{F}_{\mathrm{ex}}^{R_{n-1}}, \quad (16)$$

$$\mathbf{M}_{o_{n-1}} = \mathbf{M}_{\mathrm{CI}n} + \mathbf{M}_{\mathrm{CII}n} + \mathbf{M}_{\mathrm{d}n} + \mathbf{M}_{\mathrm{t}n} + \mathbf{M}_{\mathrm{ex}} + \mathbf{M}_{F\mathrm{ex}}, \quad (17)$$

where $\mathbf{F}_{\mathrm{ex}}^{R_{n-1}}$ is the external force expressed in the frame R_{n-1} and $\mathbf{M}_{F\mathrm{ex}}$ is the moment of external force relative to point o_{n-1}. With the help of transformation matrix, $\mathbf{F}_{\mathrm{ex}}^{R_{n-1}}$ and $\mathbf{M}_{F\mathrm{ex}}$ can be calculated by:

$$\mathbf{F}_{\mathrm{ex}}^{R_{n-1}} = {}^{R_{n-1}}\mathrm{T}_{R_G} \cdot \mathbf{F}_{\mathrm{ex}}^{R_G}, \quad (18)$$

$$\mathbf{M}_{F\mathrm{ex}} = \overrightarrow{o_{n-1} o_n}^{R_{n-1}} \times \mathbf{F}_{\mathrm{ex}}^{R_{n-1}}, \quad (19)$$

where $\mathbf{M}_{\text{ex}}$ and $\mathbf{F}_{\text{ex}}^{R_G}$ are respectively the external moment and external force expressed in the global frame.

As for the i^{th} segment of the robot, when $i = 1, \cdots n-1$, force and moment from the adjacent robot segment, i.e. the $(i+1)^{th}$ segment, should be considered. Similar to Eqns. (16) and (17), the static equilibrium equations for the i^{th} segment of the robot are:

$$\mathbf{F}_{o_{i-1}}^{R_{i-1}} = \mathbf{F}_{\text{CI}i}^{R_{i-1}} + \mathbf{F}_{\text{CII}i}^{R_{i-1}} + \mathbf{G}_{\text{d}i}^{R_{i-1}} + \mathbf{G}_{\text{t}i}^{R_{i-1}} + \mathbf{F}_{o_i}^{R_{i-1}}, \tag{20}$$

$$\mathbf{M}_{o_{i-1}} = \mathbf{M}_{\text{CI}i} + \mathbf{M}_{\text{CII}i} + \mathbf{M}_{\text{d}i} + \mathbf{M}_{\text{t}i} + \mathbf{M}_{Fo_i} + \mathbf{M}_{o_i}, \tag{21}$$

where $\mathbf{F}_{o_i}^{R_{i-1}}$ and $\mathbf{M}_{o_i}$ are respectively the force and moment applied to the i^{th} segment by the $(i+1)^{th}$ segment; $\mathbf{M}_{Fo_i}$ is the moment of force $\mathbf{F}_{o_i}^{R_{i-1}}$ relative to point o_{i-1}. Using the transformation matrix, $\mathbf{F}_{o_i}^{R_{i-1}}$ and $\mathbf{M}_{Fo_i}$ can be calculated by:

$$\mathbf{F}_{o_i}^{R_{i-1}} = {}^{R_{i-1}}\mathrm{T}_{R_i} \cdot \mathbf{F}_{o_i}^{R_i}, \tag{22}$$

$$\mathbf{M}_{Fo_i} = \overrightarrow{o_{i-1}o_i}^{R_{i-1}} \times \mathbf{F}_{o_i}^{R_{i-1}}. \tag{23}$$

Thus, the statics of the continuum robot can be described by Eqns. (16), (17), (20) and (21). As we can see from these equations, the force, the moment and the rotation angles of each segment are coupled, which means that they should be considered together.

C. Solution of the static model

According to the Euler-Bernoulli beam theory, relationship between the moment and the rotation angle for each segment of the robot can be obtained by:

$$\rho_i = \frac{M_i}{E_i I_i}, \tag{24}$$

where M_i is the value of the moment on point o_{i-1}, i.e. $M_i = z_{\mathbf{M}_{o_{i-1}}}$; E_i and I_i are respectively the Young's modulus and the moment of inertia of the i^{th} segment of the elastic tube; ρ_i is the curvature of the bending arc for the i^{th} tube. According to the geometric relationship in Fig. 3, $\rho_i = \frac{\theta_i}{L_{0i}}$.

With given driven force of the cables and the external force and moment, the rotation angle of each segments of the robot can be calculated by the static model. From Eqns. (16), (17), (20), (21) and (24), there are $3n$ independent equations and $3n$ unknowns (θ_i, $\mathbf{M}_{o_{i-1}}$ and $\mathbf{F}_{o_{i-1}}^{R_{i-1}}$ where $i = 1, \cdots n$). Optimization methods can be used to solve the $3n$ nonlinear equations. With the rotation angle θ_i, the profile of the robot can be fully obtained.

IV. Numerical Analysis and Discussion

In this section, simulations are performed to analyze the static characteristics of the continuum robot. The robot parameters and the material parameters are listed in Tab I, which are based on our previous prototypes [7].

The first simulation is performed with zero driven force and zero external load, where only gravity acts. The profile of the robot under the effect of gravity is shown in Fig. 4. The black thick line presents the fixed base, and the cyan thick lines present the movable disks. The blue thick curve presents the elastic tube. The red and green lines present the driven cables I and II. In order to validate the proposed static model, simulation results by finite element method are obtained for comparison. In this paper, a commercial software ANSYS is used to make the finite element analysis. Coordinates of the disk centers are obtained by ANSYS, which are presented by black stars in Fig. 4. Relative differences of the disk positions by these two methods are also calculated, which are smaller than 0.02%. The proposed static model has a good accuracy to describe the static behaviors of the continuum robots.

TABLE I

Robot parameters (for $i = 1, \cdots n$)

Parameter	Value	Parameter	Value
a_i	2.75 (mm)	E_i	2.5e7 (Pa)
b_i	2.75 (mm)	I_i	8.59e-12 (kg·m^2)
L_{0i}	5 (mm)	$m_{\text{t}i}$	3.3e-5 (kg)
n	10	$m_{\text{d}i}$	5.5e-5 (kg)

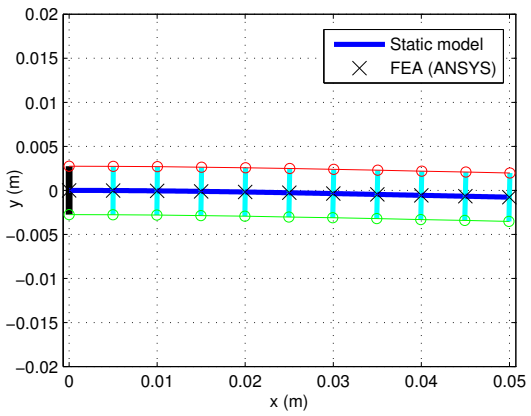

Fig. 4. Static profile of the robot under the effect of gravity (without actuation or external load).

TABLE II

Position of the robot end with different driven forces and external loadings.

$\mathbf{F}_{\text{CI}}$ (N)	$\mathbf{F}_{\text{CII}}$ (N)	$\mathbf{F}_{\text{ex}}$ (N)	O_{10} (mm)
1	3	[0 0]	A [37.1 -28.2]
1	1	[0 0]	B [50.0 -0.8]
3	1	[0 0]	C [37.9 27.4]
3	1	[0 -0.1]	D [47.7 11.4]
3	1	[0 -0.2]	E [48.9 -9.3]
3	1	[0 -0.3]	F [44.3 -21.8]

Profiles of the continuum robots can be changed by inputing different driven cable forces. Figure 5 gives an example. As shown, three shapes can be achieved by using three sets of driven forces. The rotation angle of each segment corresponding to these three shapes is presented in Fig. 7, and the corresponding positions of the robot end are listed in Tab. II. Without external loading, robot can reach point B with 1 N upper cable force and 1 N lower cable force. It can

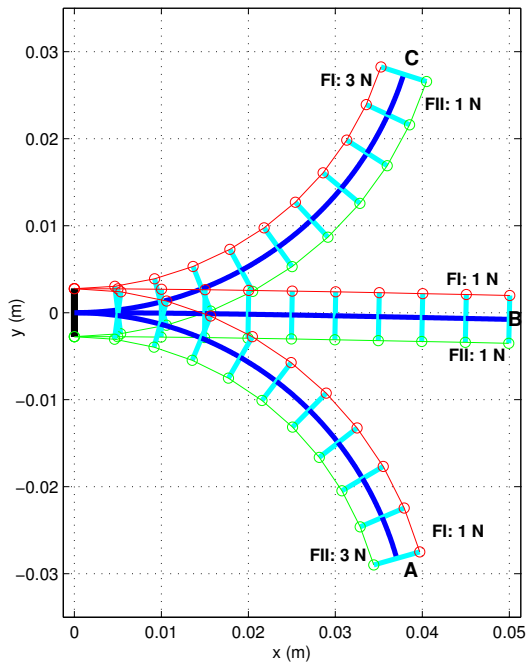

Fig. 5. Static profiles of the robot with different driven forces (zero external loading).

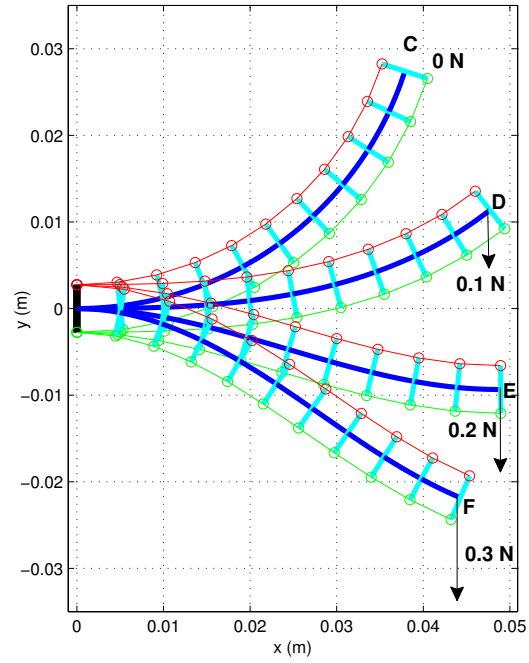

Fig. 6. Static profiles of the robot with different external loads (constant driven cable forces).

be found that the robot profile in this case is the same with that presented in Fig. 4. In fact, the profile of the continuum robot is mainly determined by the difference of the upper and lower cable forces, if there is no external loads. It means that the robot profile keeps the same by increasing/decreasing the

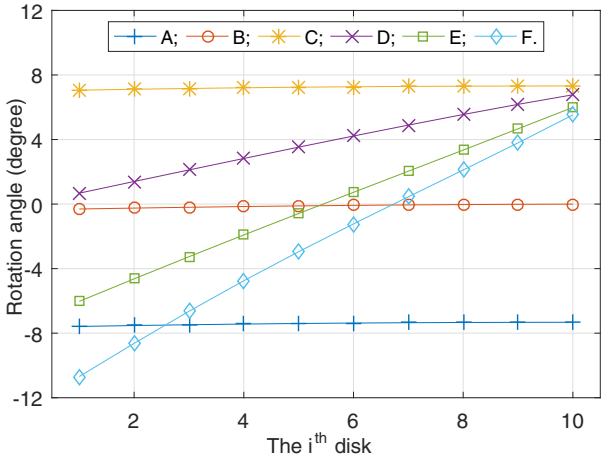

Fig. 7. Rotation angle of the i^{th} segment of the robot under different conditions.

upper and lower cable forces with the same amount, as long as the elastic tube does not exceed the limit of buckling. Robot can reach point C with 3 N upper cable force and 1 N lower cable force. While the robot end can reach point A with 1 N upper cable force and 3 N lower cable force. It should be noted that points A and C are not symmetric about x-axis (Tab. II) due to the gravity effect of the disks and tubes.

In most situations, the external loading applied to the robot end is not zero, especially when an end-effector is added. Figure 6 shows the static profiles of the robot with different external loads. The coordinates of the robot end are listed in Tab. II, and the rotation angle of each segment of the robot is shown in Fig. 7. As we can see, profiles of the continuum robots vary with the external loads, even if the driven cable forces keep the same. In addition, the rotation angle of each segment varies significantly with external loads (the D, E and F cases in Fig. 7), especially when the value of the external load becomes larger (the E and F cases in Fig. 7). For example, the rotation angles of the first 5 disks are clockwise (negative value), while the rotation angles of the last 5 disks are anti-clockwise (positive value), when the external load in y-axis is -0.2 N. The corresponding profile of the robot presents a 'S' type bending. As a comparison, the rotation angle of each segment keeps almost the same, when there is no external loading, such as cases A, B and C shown in Fig. 7, where the corresponding profile of the robot is a 'C' type bending. Therefore, external load has a significant effect on the static equilibrium of the continuum robots.

The static model of the continuum robots can be further used for the position control of the robot. With given external load and controlling cable forces, robot profiles can be obtained. Thus, position of the robot end can be calculated. On the contrary, in order to move the robot end to a desired position, the corresponding driven cable forces can be calculated through the static model. However, not all the

desired positions can be reached, i.e. there does not exist a set of controlling cable forces which can move the robot to the desired position. To solve this problem, robots with additional DOFs should be considered.

V. CONCLUSION

This research contributes on the continuum robots with application to minimally invasive surgery. This paper presents the static modeling and analysis of the single backbone continuum robots. The static model of the robots is established based on Newton-Euler method with considering the effect of gravity and external loads. A set of nonlinear equations are used to describe the coupling between the statics and kinematics, and optimization method is employed to obtain the solution of the static model. Simulation results by the proposed model are also compared with the results by finite element method. Comparison shows the difference is less than 0.02 percent, which is a good validity of the static model.

Based on the proposed static model, the static profiles of the continuum robot are calculated under different driving (cable tensions) and loading (external load) conditions. Significant effect of the external load on the static equilibrium of the robot is found, which is mainly due to the large compliance of the continuum section. In addition, the proposed static model is also useful for the positioning control of the robot. Our current and future work is on design and analysis of the position controller based on the static model presented in this paper.

ACKNOWLEDGMENT

The authors would like to thank the Shun Hing Institute of Advanced Technology,the Chinese University of Hong Kong (project SHIAE-8115049); the Hong Kong Innovative Technology Fund (ITF) (project No. ITS/019/15); and Hong Kong General Research Fund (project No.14212316) for their financial supports.

REFERENCES

[1] D. Nuss, R. E. Kelly, D. P. Croitoru, and M. E. Katz, "A 10-year review of a minimally invasive technique for the correction of pectus excavatum," *Journal of pediatric surgery*, vol. 33, no. 4, pp. 545–552, 1998.

[2] M. J. Mack, "Minimally invasive and robotic surgery," *Jama*, vol. 285, no. 5, pp. 568–572, 2001.

[3] G. Dogangil, B. Davies, and F. R. y Baena, "A review of medical robotics for minimally invasive soft tissue surgery," *Proceedings of the Institution of Mechanical Engineers, Part H: Journal of Engineering in Medicine*, vol. 224, no. 5, pp. 653–679, 2010.

[4] G. I. Barbash and S. A. Glied, "New technology and health care coststhe case of robot-assisted surgery," *New England Journal of Medicine*, vol. 363, no. 8, pp. 701–704, 2010.

[5] J. Burgner-Kahrs, D. C. Rucker, and H. Choset, "Continuum robots for medical applications: A survey," *IEEE Transactions on Robotics*, vol. 31, no. 6, pp. 1261–1280, 2015.

[6] D. B. Camarillo, C. F. Milne, C. R. Carlson, M. R. Zinn, and J. K. Salisbury, "Mechanics modeling of tendon-driven continuum manipulators," *IEEE Transactions on Robotics*, vol. 24, no. 6, pp. 1262–1273, 2008.

[7] Z. Li, M. Z. Oo, V. Nalam, V. D. Thang, H. Ren, T. Kofidis, and H. Yu, "Design of a novel flexible endoscope - cardioscope," *Journal of Mechanisms and Robotics*, vol. 8, no. 5, p. 051014, 2016.

[8] K. B. Reed, A. Majewicz, V. Kallem, R. Alterovitz, K. Goldberg, N. J. Cowan, and A. M. Okamura, "Robot-assisted needle steering," *IEEE Robotics & Automation Magazine*, vol. 18, no. 4, pp. 35–46, 2011.

[9] W. S. Rone and P. Ben-Tzvi, "Continuum manipulator statics based on the principle of virtual work," in *ASME 2012 International Mechanical Engineering Congress and Exposition*. American Society of Mechanical Engineers, 2012, pp. 321–328.

[10] Z. Li, H. Ren, P. W. Y. Chiu, R. Du, and H. Yu, "A novel constrained wire-driven flexible mechanism and its kinematic analysis," *Mechanism and Machine Theory*, vol. 95, pp. 59–75, 2016.

[11] Y.-J. Kim, S. Cheng, S. Kim, and K. Iagnemma, "Design of a tubular snake-like manipulator with stiffening capability by layer jamming," in *2012 IEEE/RSJ International Conference on Intelligent Robots and Systems*. IEEE, 2012, pp. 4251–4256.

[12] Z. Li, R. Du, and Y. Yao, "Flying octopusa ltav with wire-driven flapping wings," in *ASME 2012 International Mechanical Engineering Congress and Exposition*. American Society of Mechanical Engineers, 2012, pp. 289–295.

[13] Z. Li, R. Du, Y. Zhang, and H. Li, "Robot fish with novel wire-driven continuum flapping propulsor," in *Applied Mechanics and Materials*, vol. 300. Trans Tech Publ, 2013, pp. 510–514.

[14] Z. Li, R. Du, H. Yu, and H. Ren, "Statics modeling of an underactuated wire-driven flexible robotic arm," in *5th IEEE RAS/EMBS International Conference on Biomedical Robotics and Biomechatronics*. IEEE, 2014, pp. 326–331.

[15] N. Simaan, K. Xu, W. Wei, A. Kapoor, P. Kazanzides, R. Taylor, and P. Flint, "Design and integration of a telerobotic system for minimally invasive surgery of the throat," *The International journal of robotics research*, vol. 28, no. 9, pp. 1134–1153, 2009.

[16] M. S. Moses, M. D. Kutzer, H. Ma, and M. Armand, "A continuum manipulator made of interlocking fibers," in *Robotics and Automation (ICRA), 2013 IEEE International Conference on*. IEEE, 2013, pp. 4008–4015.

[17] K. Xu, J. Zhao, and M. Fu, "Development of the sjtu unfoldable robotic system (surs) for single port laparoscopy," *IEEE/ASME Transactions on Mechatronics*, vol. 20, no. 5, pp. 2133–2145, 2015.

[18] R. J. Webster III, J. M. Romano, and N. J. Cowan, "Mechanics of precurved-tube continuum robots," *IEEE Transactions on Robotics*, vol. 25, no. 1, pp. 67–78, 2009.

[19] M. Terayama, J. Furusho, and M. Monden, "Curved multi-tube device for path-error correction in a needle-insertion system," *The International Journal of Medical Robotics and Computer Assisted Surgery*, vol. 3, no. 2, pp. 125–134, 2007.

[20] R. J. Webster III, J. P. Swensen, J. M. Romano, and N. J. Cowan, "Closed-form differential kinematics for concentric-tube continuum robots with application to visual servoing," in *Experimental Robotics*. Springer, 2009, pp. 485–494.

[21] B. A. Jones and I. D. Walker, "Kinematics for multisection continuum robots," *IEEE Transactions on Robotics*, vol. 22, no. 1, pp. 43–55, 2006.

[22] R. J. Webster and B. A. Jones, "Design and kinematic modeling of constant curvature continuum robots: A review," *The International Journal of Robotics Research*, 2010.

[23] I. A. Gravagne and I. D. Walker, "On the kinematics of remotely-actuated continuum robots," in *Robotics and Automation, 2000. Proceedings. ICRA'00. IEEE International Conference on*, vol. 3. IEEE, 2000, pp. 2544–2550.

[24] M. Hannan and I. Walker, "Novel kinematics for continuum robots," in *Advances in Robot Kinematics*. Springer, 2000, pp. 227–238.

[25] K. Xu and N. Simaan, "Analytic formulation for kinematics, statics, and shape restoration of multibackbone continuum robots via elliptic integrals," *Journal of Mechanisms and Robotics*, vol. 2, no. 1, p. 011006, 2010.

[26] D. C. Rucker and R. J. Webster III, "Statics and dynamics of continuum robots with general tendon routing and external loading," *IEEE Transactions on Robotics*, vol. 27, no. 6, pp. 1033–1044, 2011.

[27] B. A. Jones, R. L. Gray, and K. Turlapati, "Three dimensional statics for continuum robotics," in *2009 IEEE/RSJ International Conference on Intelligent Robots and Systems*. IEEE, 2009, pp. 2659–2664.